Dirac and Majorana edge states in graphene and topological superconductors

Akhmerov, A.R.

Chapter 8

Electrically detected interferometry of Majorana fermions in a topological insulator

8.1 Introduction

There is growing experimental evidence [171–173] that the $5/2$ fractional quantum Hall effect (FQHE) is described by the Moore-Read state [5]. This state has received much interest in the context of quantum computation [8], because its quasiparticle excitations are Majorana bound states. A qubit can be stored nonlocally in a pair of widely separated Majorana bound states, so that no local source of decoherence can affect it [132]. The state of the qubit can be read out and changed in a fault-tolerant way by edge state interferometry [174–176]. This "measurement based topological quantum computation" [177] combines static quasiparticles within the Hall bar to store the qubits, with mobile quasiparticles at the edge of the Hall bar to perform logical operations by means of interferometric measurements.

The electronic correlations in the Moore-Read state involve a pairing of spin-polarized fermions, equivalent to a superconducting pairing with $p_x + ip_y$ orbital symmetry [6, 139, 178]. Such an exotic pairing might occur naturally in the Sr_2RuO_4 superconductor [147], or it might be produced artificially in p-wave superfluids formed by fermionic cold atoms [148]. Recently, Fu and Kane [130] showed how a conventional s-wave superconductor might produce Majorana bound states, if brought in proximity to a topological insulator. This class of insulators has metallic surface states with massless quasiparticles, as has been demonstrated in Bi_xSb_{1-x} alloys [161] and Bi_2Se_3 single crystals [179, 180]. The latter material is particularly promising for applications because it remains a topological insulator at room temperature. The $5/2$ FQHE, in contrast, persists only at temperatures well below 1 K [171–173].

While induced superconductivity in a topological insulator seems an attractive alternative to the FQHE for the purpose of quantum computation, one crucial difference creates a major obstacle: Quasiparticle excitations in the Moore-Read state have charge $\pm e/4$ (generated by changing the filling fraction of the half-filled Landau level), but in a superconductor the excitations have charge zero (the charge is screened by the supercon-

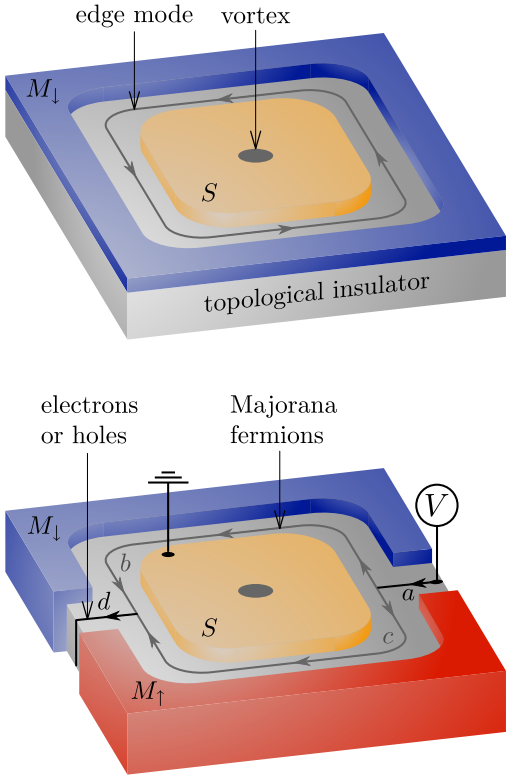

Figure 8.1: Three-dimensional topological insulator in proximity to ferromagnets with opposite polarization ($M_\uparrow$ and $M_\downarrow$) and to a superconductor (S). The top panel shows a single chiral Majorana mode along the edge between superconductor and ferromagnet. This mode is charge neutral, so it cannot be detected electrically. The Mach-Zehnder interferometer in the bottom panel converts a charged current along the domain wall into a neutral current along the superconductor (and vice versa). This allows for electrical detection of the parity of the number of enclosed vortices, as explained in the text.

ducting condensate). All known schemes [174–176] for edge state interferometry rely on electrical detection, and this seems impossible if the edge states carry no electrical current. It is the purpose of this work to propose a way around this obstacle, by showing how a pair of neutral Majorana fermions can be converted phase coherently and with unit probability into a charged Dirac fermion.

We first give a qualitative description of the mechanism of electrically detected Majorana interferometry, and then present a quantitative theory. Our key idea is to combine

edge channels of opposite chiralities in a single interferometer, by means of a magnetic domain wall. The appearance of counterpropagating edge channels in a single superconducting domain is a special feature of a topological insulator in proximity to a ferromagnet, where the propagation direction is determined by the way time reversal symmetry is broken outside of the condensate (hence by the polarization of the ferromagnets) — rather than being determined by the order parameter of the condensate (as in a $p_x \pm i p_y$ superconductor or FQHE droplet).

Refering to the lower panel of Fig. 8.1, we see that electrons or holes (with Dirac fermion operators $c_a^\dagger$ and c_a) propagate along the domain wall a until they reach the superconductor, where they are split into a pair of Majorana fermions γ_b and γ_c of opposite chirality:

$$c_a^\dagger \to \gamma_b + i\gamma_c, \quad c_a \to \gamma_b - i\gamma_c. \tag{8.1}$$

(Here we have used that $\gamma = \gamma^\dagger$, which is the defining property of a Majorana fermion.)

The Dirac-to-Majorana fermion conversion expressed by Eq. (8.1) relies on the fact that the electron or hole mode at the domain wall couples to *a pair* of Majorana modes, so that the full information encoded by the complex fermion c_a is encoded by two real fermions γ_b and γ_c. This is the essential distinction from the process of electron tunneling into a Majorana bound state [151–153, 181], which couples to *a single* Majorana fermion and can therefore not transfer the full information.

Upon leaving the superconductor the Majorana fermions recombine into an electron $c_d^\dagger$ or hole c_d depending on the number n_v of superconducting vortices enclosed by the two arms of the interferometer,

$$\gamma_b + (-1)^{n_v} i\gamma_c \to c_d^\dagger, \quad \gamma_b - (-1)^{n_v} i\gamma_c \to c_d. \tag{8.2}$$

For n_v an even integer, no charge is transfered to the superconductor, while for n_v odd a charge $\pm 2e$ is absorbed by the superconducting condensate. The conductance G, measured by application of a voltage between a point on the domain wall and the superconductor, becomes equal (in the zero-temperature, zero-voltage limit) to $G = 0$ for $n_v =$ even and $G = 2e^2/h$ for $n_v =$ odd.

8.2 Scattering matrix approach

Proceeding now to a theoretical description, we recall that the surface of a three-dimensional topological insulator, in the presence of a magnetization $\boldsymbol{M}(\boldsymbol{r})$ and superconducting order parameter $\Delta(\boldsymbol{r})$, is described by the following Hamiltonian [130]:

$$H = \begin{pmatrix} \boldsymbol{M}\cdot\boldsymbol{\sigma} + v_F\,\boldsymbol{p}\cdot\boldsymbol{\sigma} - E_F & \Delta \\ \Delta^* & \boldsymbol{M}\cdot\boldsymbol{\sigma} - v_F\,\boldsymbol{p}\cdot\boldsymbol{\sigma} + E_F \end{pmatrix}. \tag{8.3}$$

Here $\boldsymbol{p} = (p_x, p_y, 0)$ is the momentum on the surface, $\boldsymbol{\sigma} = (\sigma_x, \sigma_y, \sigma_z)$ is the vector of Pauli matrices, v_F is the Fermi velocity, and E_F the Fermi energy. The two magnetizations $M_\uparrow$ and $M_\downarrow$ in Fig. 8.1 correspond to $\boldsymbol{M} = (0, 0, M_0)$ and $\boldsymbol{M} = (0, 0, -M_0)$,

respectively. Particle-hole symmetry is expressed by the anticommutation $H\,\Xi = -\Xi H$ of the Hamiltonian with the operator

$$\Xi = \begin{pmatrix} 0 & i\sigma_y \mathcal{C} \\ -i\sigma_y \mathcal{C} & 0 \end{pmatrix}, \tag{8.4}$$

with $\mathcal{C}$ the operator of complex conjuation.

There is a single chiral Majorana mode with amplitude ψ (group velocity v_m) at a boundary between a region with a superconducting gap and a region with a magnetic gap [130]. At a domain wall between two regions with opposite signs of M_z there are two chiral Dirac fermion modes, an electron mode with amplitude ϕ^e and a hole mode with ampitude ϕ^h. The scattering matrix $S_{\rm in}(\varepsilon)$ describes scattering at excitation energy ε from electron and hole modes (along edge a) to two Majorana modes (along edges b and c in Fig. 8.1), according to

$$\begin{pmatrix} \psi_b \\ \psi_c \end{pmatrix} = S_{\rm in} \begin{pmatrix} \phi_a^e \\ \phi_a^h \end{pmatrix}. \tag{8.5}$$

Particle-hole symmetry for the scattering matrix is expressed by

$$S_{\rm in}(\varepsilon) = S_{\rm in}^*(-\varepsilon) \begin{pmatrix} 0 & 1 \\ 1 & 0 \end{pmatrix}. \tag{8.6}$$

At small excitation energies $|\varepsilon| \ll |M_z|, |\Delta|$ the ε-dependence of $S_{\rm in}$ may be neglected. (The excitation energy is limited by the largest of voltage V and temperature T.) Then Eq. (8.6) together with unitarity ($S_{\rm in}^{-1} = S_{\rm in}^\dagger$) fully determine the scattering matrix,

$$S_{\rm in} = \frac{1}{\sqrt{2}} \begin{pmatrix} 1 & 1 \\ \pm i & \mp i \end{pmatrix} \begin{pmatrix} e^{i\alpha} & 0 \\ 0 & e^{-i\alpha} \end{pmatrix}, \tag{8.7}$$

up to a phase difference α between electron and hole (which will drop out of the conductance and need not be further specified). The sign ambiguity (matrix elements $+i, -i$ or $-i, +i$) likewise does not affect the conductance.

The scattering matrix $S_{\rm out}$ for the conversion from Majorana modes to electron and hole modes can be obtained from $S_{\rm in}$ by time reversal,

$$S_{\rm out}(\boldsymbol{M}) = S_{\rm in}^T(-\boldsymbol{M}) = \frac{1}{\sqrt{2}} \begin{pmatrix} e^{i\alpha'} & 0 \\ 0 & e^{-i\alpha'} \end{pmatrix} \begin{pmatrix} 1 & \pm i \\ 1 & \mp i \end{pmatrix}. \tag{8.8}$$

The phase shift α' may be different from α, because of the sign change of $\boldsymbol{M}$ upon time reversal, but it will also drop out of the conductance.

The full scattering matrix S of the Mach-Zehnder interferometer in Fig. 8.1 is given by the matrix product

$$S \equiv \begin{pmatrix} S_{ee} & S_{eh} \\ S_{he} & S_{hh} \end{pmatrix} = S_{\rm out} \begin{pmatrix} e^{i\beta_b} & 0 \\ 0 & e^{i\beta_c} \end{pmatrix} S_{\rm in}, \tag{8.9}$$

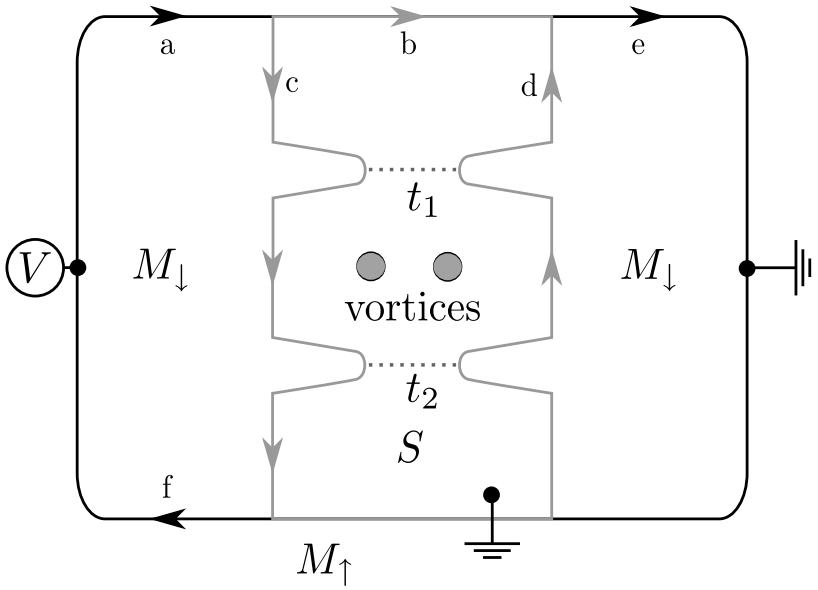

Figure 8.2: Fabry-Perot interferometer, allowing to measure the state of a qubit encoded in a pair of vortices. Black lines represent electron or hole modes at domain walls, gray lines represent Majorana modes at magnet-superconductor interface.

where β_b and β_c are the phase shifts accumulated by the Majorana modes along edge b and c, respectively. The relative phase

$$\beta_b - \beta_c = \varepsilon \delta L / \hbar v_m + \pi + n_v \pi \tag{8.10}$$

consists of three terms: A dynamical phase (proportional to the length difference $\delta L = L_b - L_c$ of the two arms of the interferometer), a Berry phase of π from the rotation of the spin-1/2, and an additional phase shift of π per enclosed vortex.

The differential conductance follows from

$$G(V) = \frac{2e^2}{h} |S_{he}(eV)|^2 = \frac{2e^2}{h} \sin^2 \left(\frac{n_v \pi}{2} + \frac{eV \delta L}{2\hbar v_m} \right). \tag{8.11}$$

As announced in the introduction, the linear response conductance $G(0)$ vanishes if the number of vortices is even, while it has the maximal value of $2e^2/h$ if the number is odd. A finite temperature T will obscure the even-odd effect if $k_B T \gtrsim \hbar v_m / \delta L$. By reducing δL, the thermal smearing can be eliminated — leaving the requirement $k_B T \ll |M_z|, |\Delta|$ as the limiting factor.

8.3 Fabry-Perot interferometer

The Mach-Zehnder interferometer can distinguish between an even and an odd number n_v of enclosed *vortices*. The next step towards measurement based topological quantum computation is to distinguish between an even and an odd number n_f of enclosed *fermions*. If n_v is odd, the parity of n_f is undefined, but if n_v is even, the parity of n_f is a topologically protected quantity that determines the state of a qubit [8]. To electrically read out the state of a qubit encoded in a pair of charge-neutral vortices, we combine the Fabry-Perot interferometer of the FQHE [175, 176] with our Dirac-Majorana converter.

The geometry is shown in Fig. 8.2. Electrons are injected in the upper left arm a of the interferometer (biased at a voltage V) and the current I is measured in the upper right arm e (which is grounded). The electron at a is split into a pair of Majorana fermions ψ_b and ψ_c, according to the scattering matrix S_{in}. A pair of constrictions allows tunneling from ψ_c to ψ_d, with amplitude t_{dc}. Finally, the Majorana fermions ψ_d and ψ_b are recombined into an electron or hole at e, according to the scattering matrix S_{out}. The resulting net current $I = (e^2/h)V(|T_{ee}|^2 - |T_{he}|^2)$ (electron current minus hole current) is obtained from the transfer matrix

$$T = S_{\text{out}} \begin{pmatrix} e^{i\beta_b} & 0 \\ 0 & t_{dc} \end{pmatrix} S_{\text{in}} \Rightarrow I = \frac{e^2}{h} V \,\text{Re}\left(e^{-i\beta_b} t_{dc}\right). \tag{8.12}$$

Notice that the current is proportional to the tunnel *amplitude*, rather than to the tunnel probability. In the low-voltage limit, to which we will restrict ourselves in what follows, the phase shift β_b vanishes and t_{dc} is real (because of electron-hole symmetry) — so I directly measures the tunnel amplitude.

In general, two types of tunnel processes across a constriction contribute to t_{dc}: A Majorana fermion at the edge of the superconductor can tunnel through the superconducting gap to the opposite edge of the constriction either directly as a fermion or indirectly via vortex tunneling [182]. Fermion tunneling typically dominates over vortex tunneling, although quantum phase slips (and the associated vortex tunneling) might become appreciable in constrictions with a small capacitance [183] or in superconductors with a short coherence length [184]. Only vortex tunneling is sensitive to the fermion parity n_f, through the phase factor $(-1)^{n_f}$ acquired by a vortex that encircles n_f fermions. Because of this sensitivity, vortex tunneling is potentially distinguishable on the background of more frequent fermion tunneling events.

The contribution to t_{dc} from fermion tunneling is simply $t_{f,1} + (-1)^{n_v} t_{f,2}$, to lowest order in the fermion tunnel amplitudes $t_{f,1}$ and $t_{f,2}$ at the first and second constriction. There is no dependence on n_f, so we need not consider it further.

To calculate the contribution to t_{dc} from vortex tunneling, we apply the vortex tunnel Hamiltonian [182] $H_i = v_i \sigma_i \sigma_i'$, where $i = 1, 2$ labels the two constrictions and v_i is the tunnel coupling. The operators σ_i and σ_i' create a vortex at the left and right end of constriction i, respectively. The lowest order contribution to t_{dc} is of second order in the tunnel Hamiltonian, because two vortices need to tunnel in order to transfer a single Majorana fermion. The calculation of t_{dc} will be presented elsewhere, but the n_v and n_f dependence can be obtained without any calculation, as follows.

Three terms can contribute to second order in H_i, depending on whether both vortices tunnel at constriction number 1 (amplitude t_1^2), both at constriction number 2 (amplitude t_2^2), or one at constriction number 1 and the other at constriction number 2 (amplitude $2t_1t_2$). The resulting expression for t_{dc} is

$$t_{dc} = t_1^2 + t_2^2 + (-1)^{n_f} 2t_1t_2, \quad \text{if } n_v \text{ is even.} \tag{8.13}$$

We see that if the two constrictions are (nearly) identical, so $t_1 \approx t_2 \equiv t$, the tunnel amplitude t_{dc} and hence the current I_{vortex} due to vortex tunneling vanish if the fermion parity is odd, while $I_{\text{vortex}} = (e^2/h)V \times 4t^2$ if the fermion parity is even.[1]

8.4 Conclusion

In summary, we have proposed a method to convert a charged Dirac fermion into a pair of neutral Majorana fermions, encoding the charge degree of freedom in the relative phase of the two Majorana's. The conversion can be realized on the surface of a topological insulator at a junction between a magnetic domain wall (supporting a chiral charged mode) and two magnet-superconductor interfaces (each supporting a Majorana mode). We found that at low voltages the Dirac-Majorana conversion is geometry independent and fully determined by the electron-hole symmetry. It allows for the electrical read-out of a qubit encoded nonlocally in a pair of vortices, providing a building block for measurement based topological quantum computation.

Much experimental progress is needed to be able to perform Majorana interferometry in any system, and the topological insulators considered here are no exception. Induced superconductivity with critical temperature $T_c > 4\,\text{K}$ has been demonstrated in BiSb [165]. It is likely that the same could be achieved in Bi_2Se_3 (the most promising realization of a three-dimensional topological insulator [179, 180]). The even-odd vortex number effect of Eq. (8.11) would then be measurable at temperatures T well below T_c — if the arms of the interferometer can be balanced to eliminate thermal smearing ($\delta L < \hbar v_m/k_B T$). This would be the first experimental mile stone, reachable with current technology. The even-odd fermion number effect of Eq. (8.13) requires coherent vortex tunneling, which is a more long-term experimental challenge [183, 184].

[1] Eq. (8.13) assumes that the number n_v of bulk vortices in between the two constrictions is even, so that n_f is well-defined. When n_v is odd, a vortex tunneling at constriction number 2 exchanges a fermion with the bulk vortices [139]. If both vortices tunnel at constriction number 2, the two fermion exchanges compensate with a phase factor of -1, but if one vortex tunnels at constriction 1 and the other at constriction 2, then the single fermion exchange prevents the transfer of a Majorana fermion across the superconductor. The resulting expression for t_{dc} therefore contains only two terms, $t_{dc} = t_1^2 - t_2^2$, if n_v is odd.